39. PV-Symposium 2024

Conference paper

https://doi.org/10.52825/pv-symposium.v1i.1205

Published: 05 Aug. 2024

A Real-Time Power Sharing Strategy for a Multi-Energy System While Considering Individual System Dynamics

Lakshimi Narayanan Palaniswamy[1], Lars Leister[1], Tassilo Zeilinger[1], Nina Munzke[1], Christian Kupper[1], and Marc Hiller[1]

[1] Karlsruhe Institute of Technology, Germany

Abstract: For a sustainable and resilient energy supply, multi-energy systems (MES) are becoming more prominent. Real-time efficient power-sharing in an MES consisting of different generation sources, uncontrollable loads, multiple storage options, and Power-to-X technologies is a challenging task. The challenge arises due to constantly fluctuating generation and load, as well as the different system dynamics of each element in the setup. Optimizing the power-sharing among the various controllable elements in an MES could be broken down into a two-level process. The top-level process, commonly known as super-ordinate control, defines the power-sharing over a longer timeframe based on load and generation forecasts and multiple other factors. The lower-level process, commonly known as sub-ordinate control, based on the inputs from the super-ordinate control and live sensor data refines the control signals of the individual elements.

This work focuses on developing a control framework for the sub-ordinate control process while considering the individual element dynamics such as dead time and rise time to a control signal. This is important as not considering differences in the system dynamics results in sub-optimal control, causing dynamic mismatches. This work proposes a simple rule-based power-splitting method backed up with individual PID regulators and Smith Predictor for each element in the MES, which are further coupled to each other for more precise and efficient control. The proposed method induces a cooperative behavior among the MES elements and improves the reaction time to a control signal while also improving the target tracking by 3-8%.

Keywords: Stationary Energy Storage, Power-to-Heat, Multi-Energy System, Real-Time Control, Optimal Power Sharing, Primary Control

1. Introduction

As a result of a global push towards the integration of distributed Renewable Energy Sources (RES) such as Photovoltaic, Wind, and other energy sources, recently Multi-Energy Systems (MES) are becoming more prominent. Forming an MES which is sometimes referred to as Smart-Energy Systems, could be defined as locally combining multiple energy sectors such as electricity, heat, cooling, transport, and so on, to interact with each other optimally [1]. Forming an MES by combining multiple sectors, especially when RES is more localized than earlier, is a crucial step towards enabling a sustainable ecosystem to live in [2], [3]. Furthermore, for higher penetration of RES in the community, Energy Storage Systems (ESS) in various forms such as electricity, heat, and others are the key [4], [5]. Due to the growing complexity of MES designing and controlling it is a challenging task [6], especially due to uncertainties of RES [7] and the operation strategy used [8], [9]. MES are often controlled through a hierarchical control

framework, where the framework could be broken down into two or sometimes three layers depending on the complexity of the system in hand [10]. Such a hierarchical control's top-level processes, commonly called super-ordinate control optimize the system operation over a longer period into the future, using forecasts and models of the MES. While doing so the superior control considers various optimization goals such as reduction of losses, reduction of storage aging, profit improvement, and others depending on the requirements defined. But, super-ordinate control does not directly control the MES, rather this task is taken up by the lower level process commonly known as sub-ordinate control. The sub-ordinate control constantly communicates with the MES and based on the directives from the super-ordinate control and live measurements defines the control signals for the MES in real-time. Such decoupling of control of MES into super-ordinate and sub-ordinate levels is necessary to reduce the influence of uncertainties caused due to RES [11].

This work focuses on the sub-ordinate controller defined above. Multiple methods are proposed in the literature to control ESSs of the MES at the sub-ordinate level. With a simple Rule-Based Control (RBC), the influence of well-known strategies such as "All or nothing" and "Low pass/ High Pass" Filtration are explored in [12]. In [13] a Dynamic Programming approach was presented, which could split the power while also reducing the overall power losses of the system. In [14] a Model Predictive Control of a Hybrid Energy Storage System connected to RES is proposed, which relies on precise Models of the system to be able to split the power in real-time. In [15], [16] well-known Fuzzy logic controllers were implemented to improve the dynamics of power flow among multiple ESS. To achieve peak shaving of an MES in islanded mode, the classic PID controller was proposed in [17]. Even computationally intensive methods such as Neural Networks and Reinforced Learning techniques are proposed in [18] for power smoothing of a distribution grid with high RES penetration. Many more similar works are available in the literature aiming at optimizing the MES operation during disturbances caused in the network due to fluctuating RES or load. However, there are very few methodologies explored focusing on controlling an MES while keeping in mind the system characteristics such as dead time and reaction time to a control signal. These characteristics of the system define how fast could the MES react to a fluctuation, such as a sudden dip in PV due to a moving cloud, thus defining its optimization potential [19]. Most of the time these system characteristics are overseen, because the research work proposing the methodology is validated for ESS designing, i.e. on a simulation level, where such system dynamics don't play a major role. Or else the ESS used for the particular research work are not commercially bought products, but rather are made as a prototype for the research work itself, thus allowing the potential to adapt the ESS characteristics for the research work. When these characteristics are ignored, there is a possibility that the sub-ordinate controller works sub-optimally, even if the super-ordinate controller defines the most optimal operation strategy possible. This work tries to prove this above statement by controlling an MES consisting of a Lithium Ion Battery (LIB), a Redox Flow Battery (RFB), and a Thermal Coupling Module (TCM) [20] defined in section 2 with the proposed methodology in section 3. The MES are subjected to a real-life measured PV power, of which the results and analysis with and without a controller are presented in section 4. Finally, the summary and outlook of the proposed method are provided in section 5.

2. Setup

2.1 System Components

The analysis of the proposed methodology in section 3 is carried out based on a real MES setup available in a Student Residence at Bruchsal, Germany. The whole setup is an AC-connected system, as shown in the schematic in Figure 1. The MES consists of two different generation sources available locally in the building, namely Photovoltaic (PV) and Wind generators. The installed PV source has a sum capacity of 220 kWp with 76% as roof-mounted and the remaining 24% as wall-mounted installations. As per the measurements done in the years 2022 and 2023, the PV is capable of generating more than 1 MWh of energy per day

during peak summer, compared to less than 50 kWh during winter. The installed wind generators are rather smaller compared to the PV with a total capacity of 10.5 kW generated by three wind generators. The student residence itself accommodates up to 150 students. The residence consumes between 330-380 kWh/day of electrical energy and 350-450 kWh/day as heat energy (based on the season) for its hot water requirement. In addition to that, the residence would also be equipped in the future with 3 charging stations for electric vehicles delivering a total of 66 kW power.

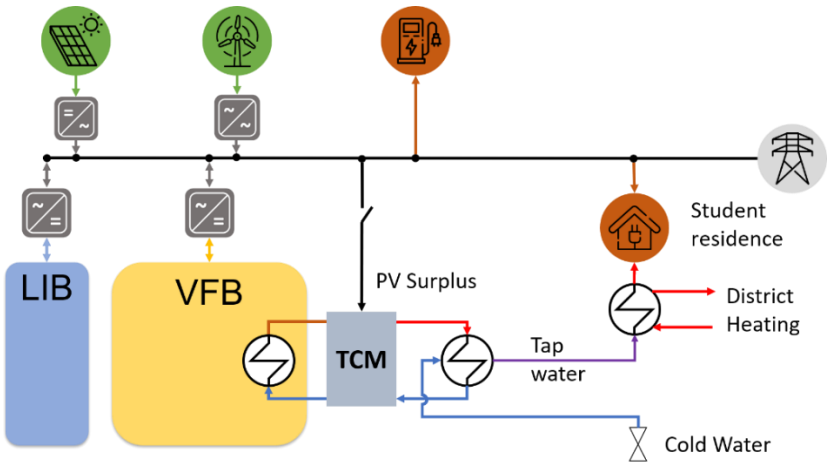

Figure 1. MES System setup schematic as available at the student residence in Bruchsal, Germany. Where LIB: Lithium Ion Battery, RFB: Redox Flow Battery, and TCM: Thermal Coupling Module.

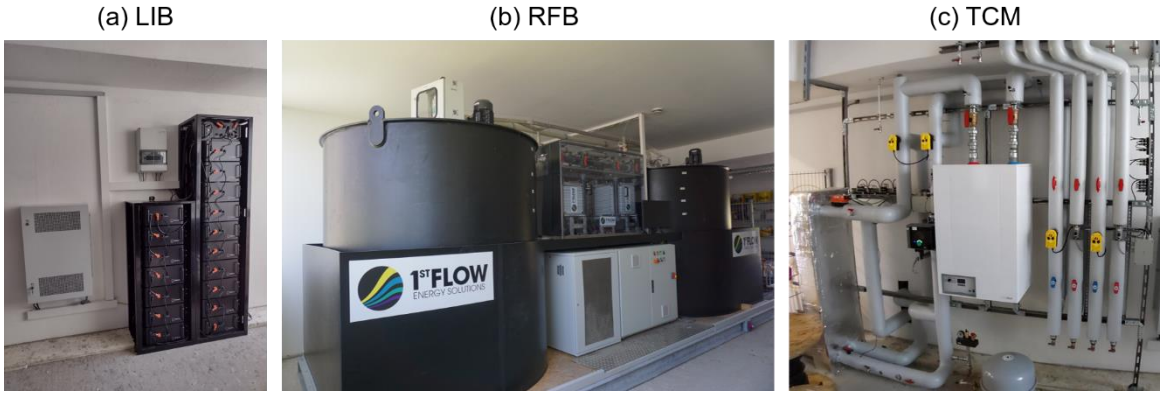

Figure 2. Controllable elements of the MES: LIB, RFB, and TCM in (a), (b), and (c) respectively

To support the RES and the load of the student residence, an innovative Hybrid Energy Storage concept is introduced, consisting of a 60 kWh Lithium Ion battery and a 120 kWh Vanadium Redox Flow Battery. The LIB has a nominal power of 30 kW whereas the RFB rates at 21 kW. The dimensioning of the ESS was done based on the results of [9]. The main aim of employing the storage system for the student residence is to improve the self-sufficiency of the building. Both LIB and RFB are commercially available systems and have been operational since 2022 (see Figure 2 (a) and (b)). The RFB is used not only as an electrical storage but also as a thermal storage, which as per the author's knowledge is a one-of-a-kind application. This dual usage of RFB is enabled through the innovative TCM [20] (see Figure 2(c)), which can convert the surplus RES electrical energy into heat and store it in the electrolyte, and extract the heat out when required. For this purpose, the electrolyte composition of the RFB is modified to be stable at higher temperatures (to 50°C) [21]. This innovation is a result of the motivation to reuse the waste heat produced by RFB operation, and also store the surplus PV

power as heat to be later used for preheating the incoming cold water to the student residence. This would not only reduce the heating requirement of the building but also improve the efficiency of the RFB.

2.2 System Characteristics

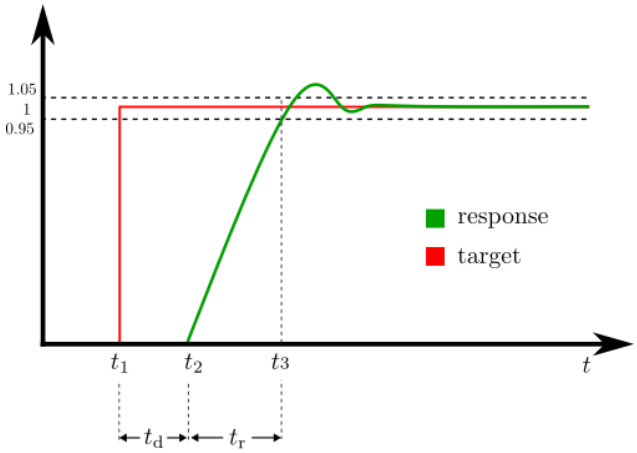

Figure 3. Visual representation of a system's response to a step signal, where $\boldsymbol{t_d}$ defines Delay time and $\boldsymbol{t_r}$ defines Rise time of the system's response

For the work presented in this paper, it is important to understand the system characteristics in terms of how the system reacts to a control signal. Figure 3 represents the general behavior of any system to a control signal. There is always some delay from the point when the control signal is generated till the point the system starts to react to it, also represented as the time between t_1 and t_2 in Figure 3, and commonly known as dead time (t_d) of the system. This is mostly caused due unavoidable communication delays between the controller and the system or could also be because of pre-requisite tasks that happen at the system's end to process the target signal [19]. The Energy Management System (EMS) used for the setup in section 2.1 is clocked at 250 ms, thus making this the minimum time delay any system would have for the setup. Furthermore, the time between t_2 and t_3 (where the system response reaches 95% of the target) in Figure 3 is defined as the rise time (t_r). This time represents how long the system takes to reach the target signal. This delay in response time is due to the internal controllers of the system, which may employ a controller of its own or have some fixed ramp rating, which is common with any ESS. These parameters of the systems are extracted through the Dynamic step test protocol defined in [22].

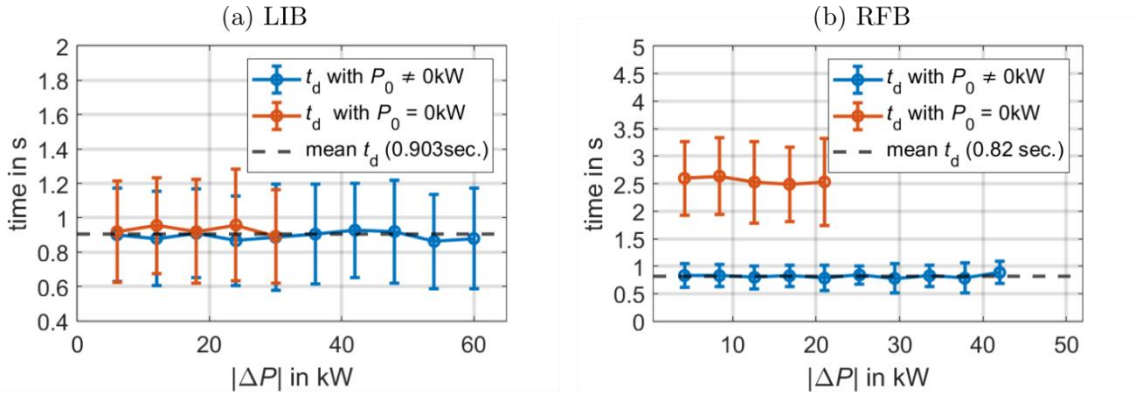

Figure 4. Dead time ($\boldsymbol{t_d}$) extracted through dynamic step test for various changes in target power ($\Delta \boldsymbol{P}$), where $\boldsymbol{P_0}$ defines the initial target power before the step change

Based on the dynamic step test results, the dead time of LIB and RFB are provided in Figure 4 (a) and (b) respectively. The results are broken down into two cases, namely: when the change in power is requested from standby, i.e. $P_0 = 0$kW, and when the ESS was already running, i.e. $P_0 \neq 0$ kW. The biggest step each ESS could make is by moving from $-P_{\mathrm{Nom}}$ to P_{Nom}. Thus, the absolute power change ($|\Delta P|$) possible for LIB is 60 kW (P_{Nom} = 30kW) and for RFB is 42 kW (P_{Nom} = 21 kW). The expectation was that t_{d} remains constant no matter what kind of change is requested to the ESS. At least LIB holds on to this expectation. But interestingly RFB has a different system dynamic. The RFB when in standby mode, reduces its pumps speeds in order to reduce standby losses. And when the system is requested to be operated, it first speeds up the pumps to bring up the required amount of flow rate of electrolyte in the stacks and then ramps up the power electronics. Thus, this results in a drastic difference on t_{d} when the system starts from standby and when the target changes while it was already under operation.

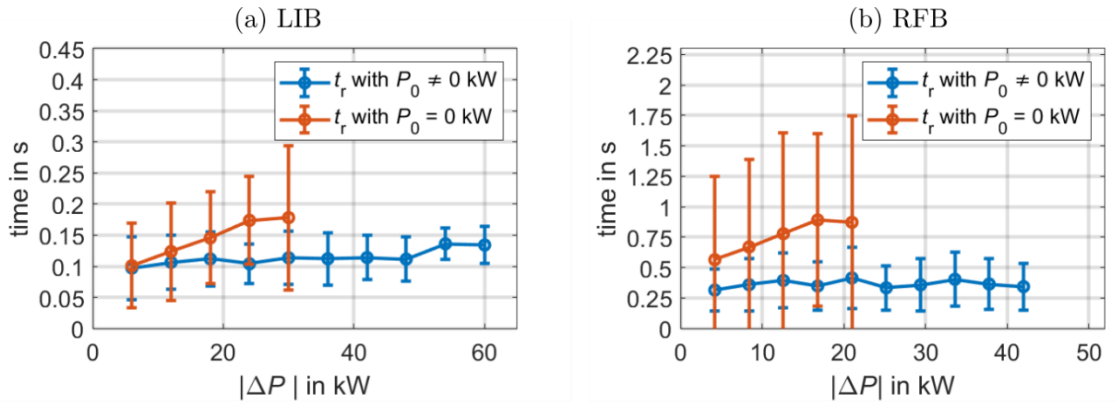

Figure 5. Rise Time ($\boldsymbol{t_{\mathrm{r}}}$) extracted through dynamic step test for various changes in target power (ΔP), where $\boldsymbol{P_0}$ defines the initial target power before the step change

Similarly, the rise time (t_{r}) of LIB and RFB are also determined through the tests as shown in Figure 5 (a) and (b) respectively. The expectation here was that the t_{r} would be linearly dependent on the absolute change in power ($|\Delta P|$). From Figure 5, it could be proved that it is so, but the interesting find through this test is that the t_{r}'s dependency to $|\Delta P|$ differs when the system was in standby compared to when it was already running. This is true for both LIB and RFB. For the TCM, tests to determine its dynamics could not be executed at the time of writing this work. The novel TCM was still in its initial construction phase, and its control framework was still being developed. For this paper it is therefore assumed that the TCM has a smaller average dead time of 0.5 sec, and similar dynamics as that of LIB. These system dynamics already give one an idea of how without a proper understanding of the system dynamics, there could be mismatches in the control of the MES. The following section defines the basics of the control concept and explains how the control concept exploits the information of system dynamics for more precise control.

3. Proposed Methodology

As defined in the previous section the aim of the real-time control algorithm for an MES is to be able to precisely split the power among all the controllable elements, while considering the differences of the individual system dynamics. In this paper, this is proposed to be achieved in two iterations, wherein the first step the power is split according to the inputs from the superordinate control, and in the second the power values are corrected according to the system dynamics, before communicating with the systems.

3.1 Inputs from super-ordinate control

Based on the load and generation forecast the super-ordinate control, generates the optimized operation strategy for economic dispatch of all the controllable elements. These inputs are regenerated by the super-ordinate control in every optimization cycle, which in practice is usually every 15 mins. The inputs are as follows:

- System operation limits: The nominal operation ranges are defined in Table 1. The LIB could operate between -30 kW to 30 kW (-ve power for charging and +ve for discharging), additionally, it cannot be operated between -500 W to 500 W. This is because operation points under 500 W are not stable, thus hindering precise control. Similarly, the RFB could be operated between -21 kW and 21 kW except for range between -7 kW and 7 kW. Here the reason is that the RFB is extremely inefficient under these operation points. Finally, the TCM being a Power-to-Heat solution could only take in electrical energy, but cannot provide it back like the other systems. Thus, its operation range is between its nominal power of -75 kW to 0 kW. Within the allowed nominal operation range the super-ordinate control generates the maximum and minimum power allowed for each system based on the optimization results. An initial draft of how the super-ordinate control works can be found here [23]. These limits could change from time to time as per the optimization done by the super-ordinate controller.

Table 1. MES absolute operation boundaries. -ve Power: Charging, +ve Power: Discharging

System	Allowed maximum charging power ($P_{\mathrm{max,CH}}$)	Allowed minimum Charging power ($P_{\mathrm{min,CH}}$)	Allowed maximum discharging power ($P_{\mathrm{max,DCH}}$)	Allowed minimum discharging power ($P_{\mathrm{min,DCH}}$)
LIB	-30kW	-0.5kW	30kW	0.5kW
RFB	-21kW	-7kW	21kW	7kW
TCM	-75kW	0kW	0kW	0kW

- System priority: Along with the operation limits, the super-ordinate control also defines a rank or priority of all the controllable elements available. This is done so that the sub-ordinate control could carry out the power splitting accordingly as explained in the next subsection 3.2. As explained, the system dealt with in this paper has three controllable elements, thus has a total of 6 plausible combinations of priority. For example, when the priority is set as LIB→RFB→TCM, then Priority (1) = LIB, Priority (2) = RFB, and Priority (3) =TCM.

3.2 Rule-Based Power-Splitting

Based on the operation limits and the priorities of the individual systems, the power splitting of the target power (P_{target}) requested happens iteratively as defined in Figure 6. At the end of the step, each system would receive its own reference target value (P_{ref}, where $\mathrm{ref} \in$ {LIB, RFB, TCM}), which it has to achieve. This power splitting process happens for every new P_{target}, i.e. every cycle of the EMS communication, or in other words in real time. For the setup used in this paper the EMS runs at a speed of 250 ms, thus the splitting also happens at this speed. This step is considered as the basic step for controlling the MES, and will be considered as base case in order to compare how the performance of control strategy proposed in this work.

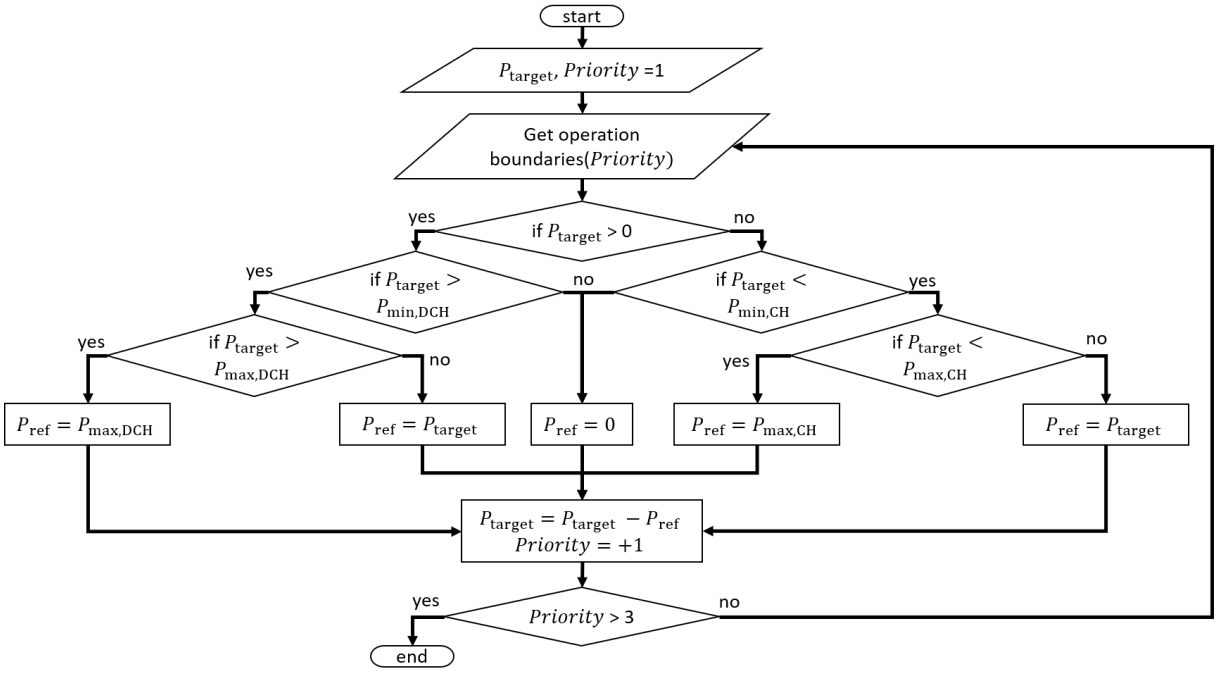

Figure 6. Flow chart of iteratively splitting the power based on rules set by the super-ordinate controller

3.3 PID Controller with Smith Predictor

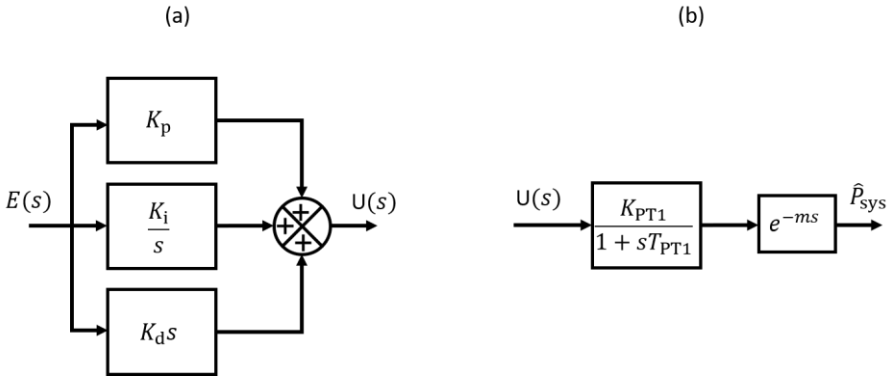

Figure 7. (a) PID Controller in its standard form in s domain, and (b) two-part plant model in s domain

The input (P_{ref}) received from the power splitting process as defined in the last subsection is further processed with a combination of a PID controller and a Smith Predictor (SP). The PID controller as defined in Figure 7 (a) could be represented in its standard parallel form (in S-domain), where its parameters K_{p}, K_{i} and K_{d} represent the proportional, integral and derivative gains. These parameters are tuned individually for each controllable element of the MES based on the Integrated Square Error (ISE) recorded during step tests

$$C(s) = \frac{U(s)}{E(s)} = K_{\text{p}} + \frac{K_{\text{i}}}{s} + k_{\text{d}}s \tag{1}$$

The PID controller could be represented as S-domain transfer function $C(s)$ (see Equation (1)) between its output $U(s)$ and the feedback error $E(s)$. Unlike traditional approaches where $E(s)$ is calculated as difference between the Plant's; i.e. the actual system's output

($P_{\mathrm{PID,sys}}$) and target (P_{ref}), the feedback is corrected further using a SP, which tries to compensate for the plant's deadtime and reaction time, in order to have a more precise control. In [24], a generalization of the SP was proposed to control linear time-invariant and time-delayed Single Input Single Output (SISO) systems. Here, it was also demonstrated how SP helps in eradicating control stability problems for system's having larger time delays. Since MES in this paper are made up of systems with variety of t_{d} and t_{r} to control signals, it only made sense to employ PID along with SP, for a much better and stable control. The SP is able to eradicate control stability with the help of a model of the plant as defined in Figure 7 (b). The model itself is broken down into two parts:

1. System reaction time (t_{r}) modeling: Here the plant could be represented as a first order lag system (PT1) and could be written down as a transfer function ($G(s)$) in the form of Equation (2). The parameters K_{PT1} and T_{PT1} define the gain and time constant of the PT1 model.

$$G(s) = \frac{K_{\mathrm{PT1}}}{1 + sT_{\mathrm{PT1}}} \tag{2}$$

2. System dead time (t_{d}) modelling: The plants dead time towards response could be model with a pure time delay represented by e^{-ms}, where m represents the modelled t_{d} of system.

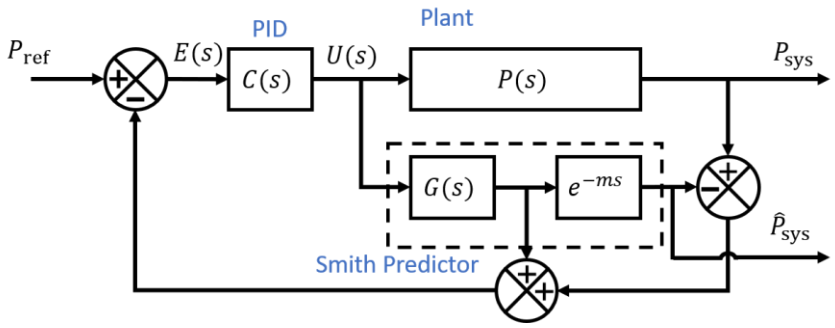

Figure 8. PID controller fitted with Smith predictor to modify the feedback loop

In this controller setup (see Figure 8) the feedback provided to PID is adapted according to the simulated response of the system with the help of a system model defined earlier. The model parameters m, K_{PT1} and T_{PT1} for each system are averaged values as per the measurements already defined earlier in Figure 4 and Figure 5. The authors would like to point out that since the systems showcase different system dynamics when P_0 = 0 kW and $P_0 \neq 0$ kW, two sets of model parameters are used for the SP, which are switched as per the system operation scenarios. The proposed controller setup of PID with SP thus produces the control signal $P_{\mathrm{PID,sys}}$ (where $sys \in$ {LIB, RFB, TCM}), which is ready to be communicated to the individual systems. Additionally, the controller also produces an estimated response of the system ($\hat{P}_{\mathrm{sys}}$) towards target $P_{\mathrm{PID,sys}}$ based on the models defined earlier.

3.4 Setpoint Correction strategy

Each element of the MES, i.e. LIB, RFB and TCM have their own set of PID controllers with an SP. These individual controllers constantly calculate the estimated responses ($\hat{P}_{\mathrm{LIB}}$, $\hat{P}_{\mathrm{RFB}}$, and $\hat{P}_{\mathrm{TCM}}$) using the system model in SP as defined in section 3.3. Based on the estimated responses and the actual target (P_{target}) for the whole MES defined in section 3.2 an estimated unused power ($\hat{P}_{\mathrm{unused}}$) is calculated as per the equation 3.

$$\hat{P}_{\mathrm{unused}} = P_{\mathrm{target}} - \hat{P}_{\mathrm{LIB}} - \hat{P}_{\mathrm{RFB}} - \hat{P}_{\mathrm{TCM}} \tag{3}$$

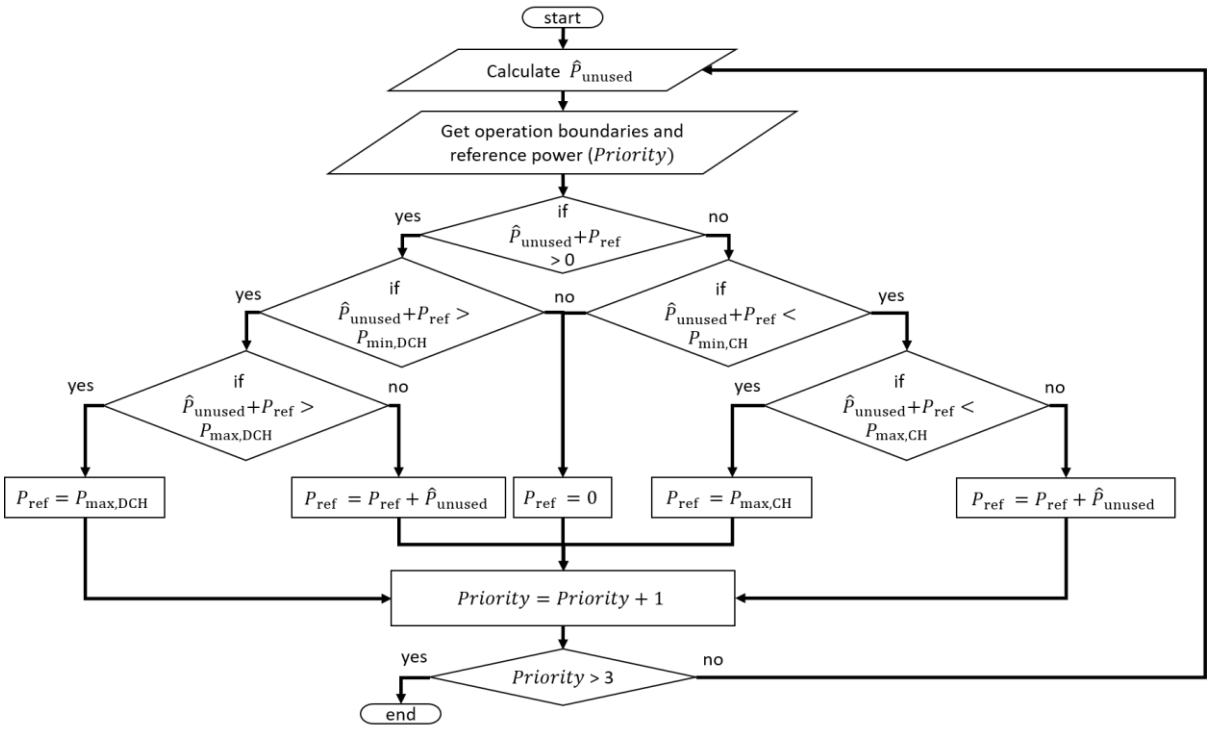

Figure 9. Setpoint correction of individual system based on $\boldsymbol{P_{\mathrm{ref}}}$ acquired from Power splitting and calculated $\boldsymbol{\hat{P}_{\mathrm{unused}}}$.

$\hat{P}_{\mathrm{unused}}$ is then compensated by reassigning the power to the elements of the MES, in addition to the power already assigned as per the power splitting process defined in Section 3.2. The aim of this step is to reduce the mismatches of control among multiple elements of MES, which not only occur due to system deadtime and or its dynamics, but also due to constant fluctuations in P_{target}. Here the strategy of compensation is to assign $\hat{P}_{\mathrm{unused}}$ to those systems of MES which can react faster to control signals so that $\hat{P}_{\mathrm{unused}}$ is compensated as soon as possible. As per the system characteristics defined in section 2.2 TCM has the least dead time, followed by RFB (when $P_0 \neq 0$ kW) and then LIB. Based on this argument, $\hat{P}_{\mathrm{unused}}$ is assigned to the MES in the fixed order TCM → RFB → LIB. The Setpoint correction step is again an iterative step similar to power splitting algorithm defined in Section 3.2. The operation ranges are defined by the super-ordinate controller, but the priority of assigning $\hat{P}_{\mathrm{unused}}$ is fixed as per the discussion above. As also shown in Figure 9, $\hat{P}_{\mathrm{unused}}$ is calculated in every iteration as per the Equation 3, and then the P_{ref} is updated for each system. This is done till the compensation process has been tried out with all the systems. Finally, the same PID controllers defined in section 3.3 are used to generate the finalized $P_{\mathrm{PID,sys}}$ target value to be communicated to the systems.

4. Results and Discussion

In order to understand the effectiveness of the proposed controller, the controller was put under test with the classical unit step test, wherein the controllable elements of MES (i.e. LIB + RFB + TCM, also represented as Sum in Figure 10) were subjected to a P_{target} = ±30 kW. A positive P_{target} could occur when the MES witnesses less to no generation, thus requiring the storage systems to provide energy instead of consuming from grid. Vice versa a negative P_{target} could occur when the MES has surplus generation of power, where the storage systems could store the energy. In order to test the system under these scenarios, the controllable elements of MES is subjected to P_{target} while having priority of RFB → LIB → TCM, and operation boundaries as defined in Table 1 expect for LIB that is limited to ±20 kW instead of ±30 kW. Note that

in the TCM has only -ve operation boundaries, which is due to the fact that it is a Power-to-Heat solution, and can only take in electrical energy.

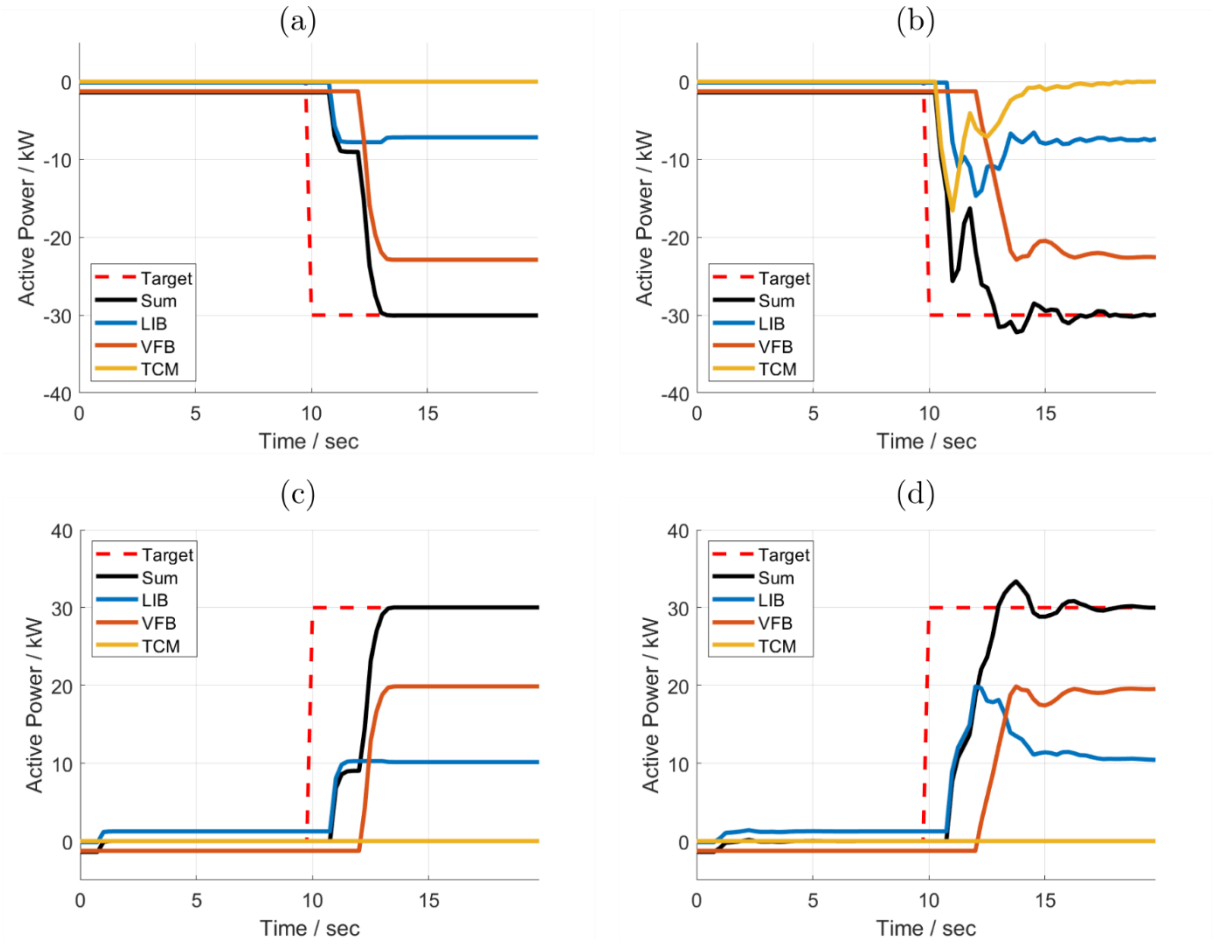

Figure 10. Test results for step of ±30 kW with allotted settling time of 8 seconds. Inputs from super ordinate controller: Priority: RFB → LIB → TCM, Case: (a), (c) without proposed controller, (b), (d) with proposed controller

Table 2. Analysis of Energy produced or delivered during unit step test on the MES controllable elements

Case	**Charge direction** Energy Consumed / Percentage of energy consumed compared to target (82.29 Wh)	**Discharge direction** Energy Delivered / Percentage of energy Delivered compared to target (82.29 Wh)
Without proposed controller	69.09 Wh / 83.96% Figure 10**Fehler! Verweisquelle konnte nicht gefunden werden.** (a)	64.40 Wh / 78.26% Figure 10 (c)
With proposed controller	76.32 Wh / 92.75% Figure 10 (b)	66.96 Wh / 81.37% Figure 10 (d)

Unit step test results are provided in Figure 10, and its statistical analysis is provided in Table 2. In Figure 10 sub-plots (a) and (c) define the base case where only the power splitting was done based on rules defined in section 3.2, whereas sub-plots (b) and (d) showcase the result of controlling LIB, RFB and TCM with the proposed control methodology. In all the cases of Figure 10 the MES is subject to a unit step for 8 sec with energy available/required of

82.29 Wh. Table 2 summarizes the amount of energy taken in (i.e. charging direction) or provided by (i.e. discharging direction) LIB, RFB and TCM together with and without the proposed controller. Visually, it could be seen in Figure 10 that the proposed controller provides higher control performance in terms of responding earlier to P_{target} by switching between the available MES elements automatically, as per their respective system dynamics. This faster response could be extremely important when an MES has to react to changes as soon as possible in order to avoid power peaks at the grid. Additionally, from Table 2 it could be inferred that the controller had up to 8% and 3% improvement in tracking P_{target} in negative direction and positive direction respectively. This goes well in hand with the fact that during the negative scenario all three controllable components of MES, i.e. LIB, RFB and TCM could participate, where as during positive direction only LIB and RFB could participate. This, showcases the strength of the concept of cooperative control among multiple elements of MES which is the basis of this work. In this result only one set of operation boundaries and priority are showcased, but the results are similar in all the other plausible cases. In order to test the theory of the proposed control strategy on real-life scenario, two test profiles are selected and the control results are simulated:

1. Daytime with heavy moving cloud, resulting in strong fluctuation (50 – 100 kW) of surplus PV available (see Figure 11)
2. Evening time, when generation is null and the mildly fluctuating (5 – 10 kW) building load must be served by the storage system (see Figure 12)

These two cases are selected to not only test the controller's performance in charging and discharging direction, but also to test its effectiveness towards strong and mild fluctuations in P_{target}. Since the proposed controller requires inputs from a super-ordinate controller, for simplicity sake a timeframe of 2 hrs is selected where these inputs remain constant. Testing the controller while the inputs from super-ordinate controller are constantly updated is out of scope for this research paper.

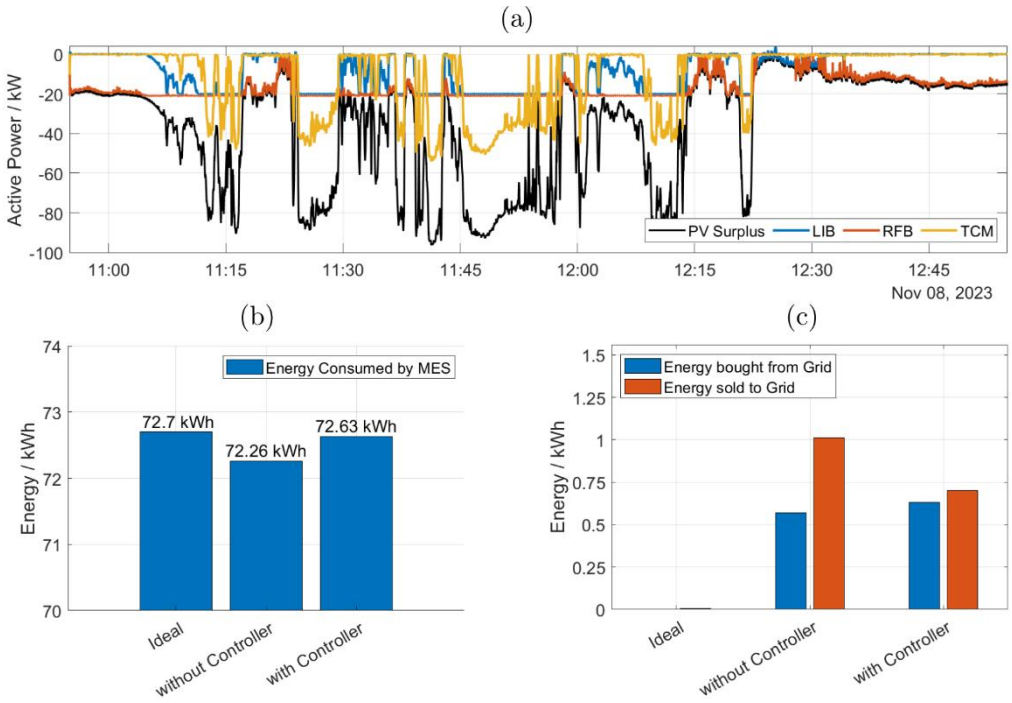

Figure 11. Result of controlling the MES during day time with surplus PV available with huge fluctuations due to constant moving clouds

Figure 11 (a) showcases the power profile of the Surplus PV (or P_{target}) available during the time in black colored line, whereas the power profile in blue, orange and yellow define that

of LIB, RFB and TCM respectively. The showcased test runs for 2 h, where the operation boundaries and priority remain the same as defined for the unit step test. Figure 11 (b) visualizes the energy consumed by the MES in the form of a bar chart. Here "Ideal" case is defined when P_{target} is split as defined in section 3.2 and the systems react ideally to it, i.e. with 0 t_{d} and t_{r}, or in other words ideal tracking of P_{target}. The case "without controller" is similar to "ideal" case, but here the systems react with its individual t_{d} and t_{r} as defined in section 2.2. The case "with controller" is an extension to the previous, but here the proposed control strategy is employed. In Figure 11 (b), it could be seen that LIB + RFB + TCM were able to charge up till 72.67 kWh when operated with the controller, which is 0.37 kWh more than when it was operated without the controller. This goes well in hand with the motivation to store as much surplus as possible into the storage systems despite of the fluctuations and control mismatches. This, extra energy stored would indeed improve the self-sufficiency of the MES when used later during no generation period. In order to analyze at what cost this improvement was made, Figure 11 (c) analyzes the grid exchanges during the test period. Here the energy fed into the grid was successfully reduced from 1.01 kWh to 0.689 kWh (31.1% decrease). At the same time the amount of energy bought from the grid during the control process had increased by 13% from 0.576 kWh (without controller) to 0.6546 kWh (with controller).

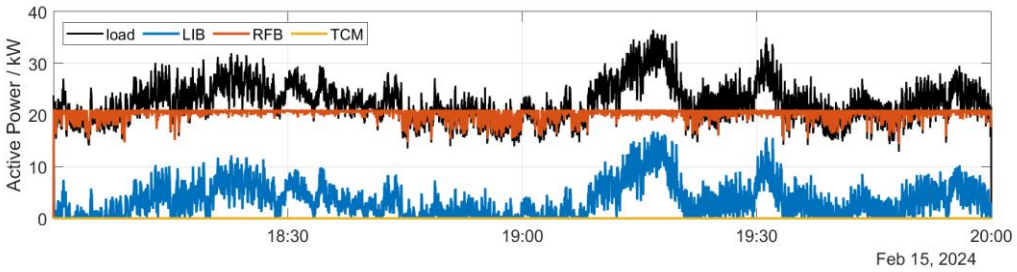

Figure 12 Result of controlling the MES during evening, where the storage systems must respond to the building load requirement

Figure 12 showcases the result of MES operation during the discharge phase. Here the authors are making an assumption, that the energy stored in the storage systems was completely from renewable sources. The proposed controller was able to serve 100% of the load (45.02 kWh), whereas without controller it was 99,86%, which corresponds to a difference of 0,06 kWh. This also goes well in hand with the motivation to supply the building load completely with cheaper energy stored from the PV. Here, controlling the storage system came at a cost of losing some of the stored energy into the grid. This had increased by 7%, i.e. from 0.788 kWh (without controller) to 0.843 kWh (with controller). Energy taken from the grid for the control process was nearly the same in both the cases. At present in Germany feed-in tariff of PV energy is 0.05 €/kWh (for PV systems above 100 kWp) when only the excess PV is stored into the grid [25], which is relevant to the setup of this work. At the same time the energy taken from the grid costs 0.28 €/kWh as per the electricity contract of the student residence. Thus, it can be said that the energy stored into the storage systems costs (0.28 €/kWh – 0.05 €/kWh =) 0.23 €/kWh. This is not completely true, and is much more complex to calculate, as the cost of energy stored in to the storage systems dependent on the losses occurred during the operation of the system, which are in turn dependent on the operation points themselves. But since the test run is only for 2 hrs, the difference between actual cost of energy stored in the system and the calculated 0.23 €/kWh is negligible, thus ignored. Thus, in test case 1 the controller was able to gain 0.085 € by storing 0.37 kWh more than the base cases, but had lost 0.0145 € by taking 0.063 kWh more energy from the grid to do so. Thus overall, the proposed controller was still better by 0.099 €. Similarly, in test case 2, the controller was able to serve 0.08 kWh more energy compared to the base case which leads to a gain of 0.0184 €, but had to lost 0.0172 € by selling 0.075 kWh more energy to the grid. Here, the proposed controller did not bring out much of an advantage as the overall gain is less than 1 Cent. This could also be argued that it is not because of the controller because only seldomly both LIB and RFB were actively participating in the controlling process together, thus losing the advantage of using

multiple elements in supporting each other's operation. The financial gains observed from the proposed controller's experimental trials are minimal, largely due to the limited time-frame of 2 hrs. When the time frame is extended beyond 2 hrs the inputs from the super-ordinate controller is constantly updated, making the evaluation a much challenging task. Additionally, the load fluctuations observed over the course of a year are not always consistent to the experiments showcased in this paper. Consequently, it can be theoretically estimated that over a year's time, the controller will not produce extremely high financial gains, at least when considered in the context of a simple German household electricity price scenario. It should be noted that the results presented in this work are based on simulations and that the actual performance may be higher in reality. However, this has not yet been tested and is planned as a future work. Nevertheless, the proposed controller is a software solution for addressing dynamic mismatch losses that arise during the control of elements of an MES. It can be readily adopted by any other application, with only minor modifications to the PID control parameters and the models of the systems under consideration (see section 3.3).

5. Conclusion and outlook

This paper considers a real-life Multi Energy System (MES) consisting of a Lithium Ion Battery, a Vanadium Redox Flow Battery, and a Thermal Couple Module (Power-to-Heat solution) [20] used to serve a student residence with locally available Photovoltaic and wind energy sources. When employing such diverse systems in an MES, it is difficult to control all the systems together due to their unique system dynamics: dead-time and rise-time. These system dynamics, could most of the time result in control mismatches, especially when the target power keeps fluctuating. This paper tries to solve this problem with individual PID controllers backed up with a Smith Predictor to obtain stable control despite of different system dynamics. The proposed controller works as a sub-ordinate controller and abides by the operation boundaries and priority of MES elements set by the super-ordinate control. Firstly, the controller was put to test under step tests, where the controller was not only able to react faster to changes in target, but also track the target power 3-8 % better. It was also found that the higher the number of controllable elements available in an MES, the higher the performance improvement is likely to be. This goes hand in hand with the motivation to negate the effect of different dead times and rise times of the MES elements by enabling cooperative control among each other. Secondly, to test the performance improvement as well as the economical effectiveness of the proposed controller under real-life situations, the controller was put to test under two cases: 1. Daytime with highly fluctuating PV surplus, due to moving cloud, and 2. Night time with mildly fluctuating building load where the storage systems discharge. In the first case, the MES was able to store 0.37 kWh (or 0.5%) more than the case without the proposed controller, by reducing up-to 30% of the energy sold to the grid and having 13% increase in energy bought from the grid. By applying current feed-in tariff and electricity prices of normal residence in Germany, the controller was able to gain 0.099 € in 2 hrs. In the second case, the controller was able to achieve 100% of the load energy requirement, but in doing so it lost part of the energy stored to the grid, thus nullifying the economic advantage compared to the case without a controller. This is due to the fact that not all the elements were participating together in case 2, thus losing the cooperative advantage of the system elements, which the proposed controller tries to exploit. With this it could be estimated that the financial gains over a year would also not be significantly huge, at least while considering a simple German household electricity tariff. Nonetheless, the results provided in this paper are on simulation level, and it is expected that in real-life operation the advantages might improve. This is yet to be tested by the authors and is planned in the near future. Thus, it could be concluded that including system dynamics in controlling the elements of an MES does have a positive effect of tracking the load more effectively. When considering a constant electricity tariff, financial gain is low. The larger the differences between the individual dead times are, the more advantageous the shown setup becomes. The financial gains could also see a major improvement in dynamic price tariffs, or peak shaving applications, where the peak power has drastically high price. In all cases, the

proposed methodology is a software solution to fine tune the controlling an MES, which provides a financial gain at no initial investment. To be able to adapt the provided solution for any other application the PID controllers and the system models used would have to be updated.

Data availability statement

Data could be provided on request.

Underlying and related material

No earlier contributions from the author are related to this work.

Author contributions

Lakshimi Narayanan Palaniswamy: Conceptualization, Methodology, Software, Investigation, Writing-Original Draft, Visualization, Resources. **Lars Leister**: Conceptualization, Writing - Review & Editing. **Tassilo Zeilinger**: Software, Investigation, Validation. **Nina Munzke**: Writing - Review & Editing, Supervision, Project administration, Funding acquisition. **Christian Kupper**: Writing - Review & Editing, Supervision, Project administration. **Marc Hiller**: Project administration, Funding acquisition.

Competing interests

The authors declare that they have no known competing financial interests or personal relationships that could have appeared to influence the work reported in this paper.

Funding

The results presented here were generated within the “BiFlow” project (funding code: 03EI3025A), funded by the Federal Ministry for Economic Affairs and Climate Action (BMWK), Germany**.**

Acknowledgement

This work contributes to the research performed at KIT Battery Technology Center**.** The authors thank the project partners for their support in planning and installation of system, and the project management organization Jülich (PTJ) and the BMWK, Germany.

References

[1] P. Mancarella, “MES (multi-energy systems): An overview of concepts and evaluation models,” *Energy*, vol. 65, pp. 1–17, Feb. 2014, doi: 10.1016/j.energy.2013.10.041.

[2] E. Guelpa, A. Bischi, V. Verda, M. Chertkov, and H. Lund, “Towards future infrastructures for sustainable multi-energy systems: A review,” *Energy*, vol. 184, pp. 2–21, Oct. 2019, doi: 10.1016/j.energy.2019.05.057.

[3] W. Huang, N. Zhang, J. Yang, Y. Wang, and C. Kang, “Optimal Configuration Planning of Multi-Energy Systems Considering Distributed Renewable Energy,” *IEEE Trans. Smart Grid*, vol. 10, no. 2, pp. 1452–1464, Mar. 2019, doi: 10.1109/TSG.2017.2767860.

[4] A. Bartolini, F. Carducci, C. B. Muñoz, and G. Comodi, “Energy storage and multi energy systems in local energy communities with high renewable energy penetration,” *Renew. Energy*, vol. 159, pp. 595–609, Oct. 2020, doi: 10.1016/j.renene.2020.05.131.

[5] S. Mazzoni, S. Ooi, B. Nastasi, and A. Romagnoli, “Energy storage technologies as techno-economic parameters for master-planning and optimal dispatch in smart multi energy systems,” *Appl. Energy*, vol. 254, p. 113682, Nov. 2019, doi: 10.1016/j.apenergy.2019.113682.

[6] S. Pfenninger, A. Hawkes, and J. Keirstead, “Energy systems modeling for twenty-first century energy challenges,” *Renew. Sustain. Energy Rev.*, vol. 33, pp. 74–86, May 2014, doi: 10.1016/j.rser.2014.02.003.

[7] A. Starosta, P. Jhaveri, N. Munzke, and M. Hiller, *Wirtschaftlicher Einfluss von PV-Prognose-Ungenauigkeiten auf eine Ladeinfrastruktur für Unternehmensparkplätze*. PV Symposium, 2022.

[8] N. Munzke, F. Büchle, A. Smith, and M. Hiller, “Influence of Efficiency, Aging and Charging Strategy on the Economic Viability and Dimensioning of Photovoltaic Home Storage Systems,” *Energies*, vol. 14, no. 22, Art. no. 22, Jan. 2021, doi: 10.3390/en14227673.

[9] N. Munzke, B. Schwarz, F. Büchle, and M. Hiller, “Evaluation of the efficiency and resulting electrical and economic losses of photovoltaic home storage systems,” *J. Energy Storage*, vol. 33, Jan. 2021, doi: 10.1016/j.est.2020.101724.

[10] J. Li *et al.*, “Control method of multi-energy system based on layered control architecture,” *Energy Build.*, vol. 261, p. 111963, Apr. 2022, doi: 10.1016/j.enbuild.2022.111963.

[11] J. He, C. Shi, T. Wei, X. Peng, and Y. Guan, “Hierarchical optimal energy management strategy of hybrid energy storage considering uncertainty for a 100% clean energy town,” *J. Energy Storage*, vol. 41, p. 102917, Sep. 2021, doi: 10.1016/j.est.2021.102917.

[12] A. L. Allegre, A. Bouscayrol, and R. Trigui, “Influence of control strategies on battery/supercapacitor hybrid Energy Storage Systems for traction applications,” in *2009 IEEE Vehicle Power and Propulsion Conference*, Sep. 2009, pp. 213–220. doi: 10.1109/VPPC.2009.5289849.

[13] Z. Song, H. Hofmann, J. Li, X. Han, and M. Ouyang, “Optimization for a hybrid energy storage system in electric vehicles using dynamic programing approach,” *Appl. Energy*, vol. 139, pp. 151–162, Feb. 2015, doi: 10.1016/j.apenergy.2014.11.020.

[14] H. Chen, R. Xiong, C. Lin, and W. Shen, “Model predictive control based real-time energy management for hybrid energy storage system,” *CSEE J. Power Energy Syst.*, vol. 7, no. 4, pp. 862–874, Jul. 2021, doi: 10.17775/CSEEJPES.2020.02180.

[15] B. Bohnet *et al.*, “Hybrid Energy Storage System Control for the Provision of Ancillary Services,” in *International ETG Congress 2017*, Nov. 2017, pp. 1–6. Accessed: Feb. 12, 2024. [Online]. Available: https://ieeexplore.ieee.org/document/8278764/authors#authors

[16] M. J. van Jaarsveld and R. Gouws, “An Active Hybrid Energy Storage System Utilising a Fuzzy Logic Rule-Based Control Strategy,” *World Electr. Veh. J.*, vol. 11, no. 2, Art. no. 2, Jun. 2020, doi: 10.3390/wevj11020034.

[17] S. Chapaloglou *et al.*, “Smart energy management algorithm for load smoothing and peak shaving based on load forecasting of an island’s power system,” *Appl. Energy*, vol. 238, pp. 627–642, Mar. 2019, doi: 10.1016/j.apenergy.2019.01.102.

[18] E. Reihani, M. Motalleb, R. Ghorbani, and L. Saad Saoud, “Load peak shaving and power smoothing of a distribution grid with high renewable energy penetration,” *Renew. Energy*, vol. 86, pp. 1372–1379, Feb. 2016, doi: 10.1016/j.renene.2015.09.050.

[19] J. Weniger, T. Tjaden, J. Bergner, and V. Quaschning, “Dynamic mismatch losses of grid-connected PV-battery systems in residential buildings,” *J. Energy Storage*, vol. 13, pp. 244–254, Oct. 2017, doi: 10.1016/j.est.2017.07.011.

[20] N. Munzke, C. Kupper, and M. Mast, “Thermisches Koppelmodul, thermisches Koppelungssystem und Verfahren zur Wärmeübertragung zwischen mindestens einem elektrischen Energiespeicher und mindestens einem Wärmeabnehmer,” German Patent 10 2022 121 873 [Online], Mar. 14, 2024, Available: DPMAregister

[21] N. V. Roznyatovskaya *et al.*, “Adjustment of Electrolyte Composition for All-Vanadium Flow Batteries and Its Effect on the Thermal Stability of Electrolyte for Positive and Negative Half-Cells,” *Energy Technol.*, vol. 12, no. 1, p. 2300739, 2024, doi: 10.1002/ente.202300739.

[22] “Efficiency guideline for PV storage systems,” *BVES Bundesverb. Energiespeicher*, Apr. 2019.

[23] L. N. Palaniswamy, N. Munzke, C. Kupper, and M. Hiller, “Optimized Energy Management of a Solar and Wind Equipped Student Residence with Innovative Hybrid Energy Storage and Power to Heat Solutions,” presented at the International Renewable Energy Storage Conference (IRES 2022), Atlantis Press, May 2023, pp. 363–382. doi: 10.2991/978-94-6463-156-2_24.

[24] R. Sanz, P. García, and P. Albertos, “A generalized smith predictor for unstable time-delay SISO systems,” *ISA Trans.*, vol. 72, pp. 197–204, Jan. 2018, doi: 10.1016/j.isatra.2017.09.020.

[25] “Recent Facts about Photovoltaics in Germany - Fraunhofer ISE,” Fraunhofer Institute for Solar Energy Systems ISE. Accessed: Mar. 07, 2024. [Online]. Available: https://www.ise.fraunhofer.de/en/publications/studies/recent-facts-about-pv-in-germany.html